Comparison of Technetium-99m-Q3 and Thallium-201 for Detection of Coronary Artery Disease in Humans

Myron C. Gerson, Jennifer Lukes, Edward Deutsch, Danuta Biniakiewicz, Lee C. Washburn, Abdelhamid H. Elgazzar, R. C. Elder and Richard A. Walsh

From the Division of Cardiology, Department of Internal Medicine; E. L. Saenger Radioisotope Laboratory; Departments of Radiology and Chemistry, University of Cincinnati, Cincinnati, Ohio; and Mallinckrodt Medical Inc., St. Louis, Missouri

Technetium-99m-Q3 is a myocardial imaging agent that produces prompt myocardial visualization in humans. **Methods:** In 19 patients with angiographic coronary artery disease, 2 patients with no angiographic coronary artery stenosis greater than 50% of the luminal diameter and 6 healthy volunteers, exercise and resting myocardial imaging were performed with ^{99m}Tc-Q3 and also with ^{201}Tl. Technetium-99m-Q3 imaging began 15 min after injection at rest and with exercise, in a complete imaging sequence that required less than 100 min. **Results:** Overall accuracy for coronary disease detection was 78% (21 true-positive or true-negative studies among 27 study participants) by tomographic thallium imaging versus 89% for ^{99m}Tc-Q3 tomographic imaging (p = ns). Accuracy for detection of individual coronary stenoses was 75% (61 true-positive or true-negative coronary segment classifications among 81 total coronary segments) for ^{201}Tl imaging and 83% for ^{99m}Tc-Q3 imaging (p = ns). **Conclusions:** Technetium-99m-Q3 when used in a rest-exercise sequence that can be completed in 100 min appears to provide comparable diagnostic accuracy to ^{201}Tl for overall coronary disease detection and detection of individual coronary artery stenoses.

Key Words: myocardial perfusion imaging; technetium-99m-Q3

J Nucl Med 1994; 35:580–586

In 1981, Deutsch et al. described the first in a series of ^{99m}Tc complexes with uptake in the myocardium (*1*). Technetium-99m-dichlorodimethylphosphinoethane (DMPE) provided a very early example of ^{99m}Tc myocardial perfusion images in humans (*2*). Since that time, numerous advances have occurred in the development of ^{99m}Tc myocardial imaging agents, including the investigation and clinical availability of ^{99m}Tc-sestamibi, an isonitrile complex (*3,4*), and ^{99m}Tc-teboroxime, a boronic acid adduct (*5–8*). These ^{99m}Tc agents yield superior myocardial images compared to ^{201}Tl as a result of the higher gamma energy of ^{99m}Tc (*3*). However, these newer imaging agents also have important limitations of their own. Both have a high level of hepatic activity early following injection which can interfere with imaging of the inferior and apical left ventricular walls (*3,7,8*).

Several newer cationic ^{99m}Tc myocardial imaging agents are currently being tested, including tetrofosmin (*9–11*), a diphosphine complex; furifosmin or Q12 (*12,13*) and Q3. Structurally, the Q complexes differ from the diphosphine complexes, tetrofosmin and DMPE because the Q complexes contain monophosphine ligands as well as a distinct Schiff base ligand. Therefore, these Q series tracers are more accurately described as mixed ligand complexes. The monophosphine ligands of ^{99m}Tc-Q3 and ^{99m}Tc-Q12 are identical (i.e., tris(3-methoxy-1-propyl)phosphine), but the Schiff base ligand of ^{99m}Tc-Q12 contains a pair of extra furan rings. Initial reports suggest that tetrofosmin, Q3 and Q12 may clear more rapidly from the liver compared to currently available clinical ^{99m}Tc myocardial imaging agents (*9,11,12*). If confirmed, accelerated hepatic clearance of these newer ^{99m}Tc imaging agents should facilitate early myocardial imaging following tracer injection, resulting in improved convenience for patients. Technetium-99m-Q12 and ^{99m}Tc-Q3 show minimal evidence of myocardial washout (*11,13,14*). Therefore, separate exercise and rest injections are required.

To date, no studies have compared ^{99m}Tc-tetrofosmin to ^{99m}Tc-Q12 or Q3. Technetium-99m-Q12 is available as an "instant kit" (*15*), but no similar kit has been developed as yet for ^{99m}Tc-Q3. It has been speculated that ^{99m}Tc-Q12 may clear more rapidly from the liver in comparison to ^{99m}Tc-Q3 (*16*), but that background activity in the lung may be lower for ^{99m}Tc-Q3 compared to ^{99m}Tc-Q12. However, no direct comparisons of these two tracers in the same patients have been published.

Presently, no single-photon emitting myocardial imaging agent has been shown to provide more accurate detection of coronary artery disease (CAD) in comparison to ^{201}Tl. Therefore, the purpose of the present investigation was to directly compare ^{99m}Tc-Q3 images to ^{201}Tl images in patients with documented angiographic coronary anatomy.

Received Oct. 8, 1993; revision accepted Jan. 20, 1994.

For correspondence or reprints contact: Myron C. Gerson, MD, University of Cincinnati, Division of Cardiology, Mail Location #542, Cincinnati, OH 45267-0542.

METHODS

Study Population

The study population consisted of 21 patients with known or suspected CAD and 6 healthy volunteers. Each study participant completed an informed consent statement approved by the Institutional Review Board of the University of Cincinnati Medical Center. Patients with known or suspected CAD were consecutively entered into the study provided that: (1) they were referred by a physician for exercise ^{201}Tl myocardial imaging; (2) coronary arteriography was completed or scheduled at the time of study entry; (3) the patient agreed to and the referring physician concurred with study participation; and (4) no revascularization procedure or cardiac event occurred within the time frame, including the two imaging procedures and coronary arteriography. No patient was excluded from study participation based on scintigraphic or angiographic findings. The mean interval between coronary arteriography and ^{99m}Tc-Q3 imaging was 35 ± 13 wk. Patients with known or suspected coronary disease included 11 men and 10 women with a mean age of 60 ± 2 yr. Among the 21 known or suspected coronary patients, 10 patients were hypertensive, 8 had known diabetes mellitus, 7 had hyperlipidemia and 2 smoked a tobacco product. Calcium antagonists were used by nine patients, beta-adrenergic blockers in three patients and long-acting nitrates in six patients. No attempt was made to discontinue the use of antianginal drugs for exercise testing, but patients used the same medication and dose at the time of thallium imaging and ^{99m}Tc-Q3 imaging.

The group of 6 asymptomatic healthy volunteers included 2 men and 4 women with a mean age of 29 ± 3 yr. Volunteers were nonsmokers with no history of diabetes mellitus, hypertension or hyperlipidemia. The volunteers were using no medication.

Exercise Thallium Tomography

Exercise ^{201}Tl tomographic testing was performed and interpreted by standard methods (*17*). In the fasting state, each study participant walked on a motor-driven treadmill according to a modified Bruce protocol (*18*). With continuous electrocardiographic and intermittent blood pressure monitoring, each participant walked until limiting symptoms occurred. Thallous chloride (2.0–3.0 mCi) was injected intravenously at peak exercise and the participant continued exercising for an additional minute.

Tomographic thallium imaging was started 10–15 min following thallium injection. Tomographic thallium images were acquired with a Siemens Orbiter large field of view gamma camera (Siemens Medical Systems, Inc., Iselin, NJ) equipped with a low-energy, all-purpose collimator. The photoenergy peaks were centered around the 83-keV and 167-keV emissions of ^{201}Tl using a 20% window. Images were acquired for 30 sec at 32 stops over a circular orbit from the 45° right anterior oblique to the 45° left posterior oblique position. The data were collected on a 64 × 64 matrix on a MEDASYS pinnacle computer (MEDASYS, Inc., Ann Arbor, MI). Following a 5-point prefiltering sequence, the plane projections were filtered with a Butterworth filter with an order of 5 and then backprojected. Tomographic images were displayed on radiographic film as a series of 6.5-mm-thick slices oriented in the short-axis and vertical and horizontal long-axis projections.

In patients with uniform or nearly uniform myocardial distribution of ^{201}Tl on the exercise images, redistribution tomographic images were acquired (without reinjection) 3 to 4 hr later. In patients with nonuniform exercise distribution of thallium activity in the left ventricular myocardium, reinjection with 1 mCi of ^{201}Tl was performed at 3–4 hr postexercise, after which reinjection tomographic images were acquired beginning 20–30 min later (*17*). Thallium reinjection was used in 18 of the 19 patients with angiographic CAD, but not in the patients with normal coronary arteriograms nor in the healthy volunteers. No indication of the presence or absence of thallium reinjection was present on the films submitted for interpretation in blinded fashion.

Preparation of ^{99m}Tc-Q3

Trans(N,N′-ethylenebis(acetylacetoneimine)bis(tris(3-methoxy-1-propyl)phosphine) ^{99m}Tc(III) (^{99m}Tc-Q3) was prepared as follows. N,N′-ethylenebis(acetylacetoneimine) (H_2acac_2en, 15–25 mg in 0.1–0.2 ml of ethanol) was combined with KOH (0.03 ml of 1 *M* solution in 50% ethanol) and $Na^{99m}TcO_4$ (1–2 ml containing 80–120 mCi) in a 5-ml sterile vial. The solution was deaerated with a vigorous stream of oxygen-free argon for 10–15 min. At the same time, a solution of $SnCl_2$ in ethanol (2–3 mg/ml) was prepared by first deaerating the ethanol, then adding the $SnCl_2$, and finally stoppering the vial immediately to ensure anaerobic conditions. Under anaerobic conditions, 10–20 μl of the $SnCl_2$ solution was added to the reaction vial, and the solution was heated for 15 min at 70–90°C. The air-sensitive product formed, ($[^{99m}Tc(V)(acac_2en)O]^+$) was assayed for purity by reversed-phase high-performance liquid chromatography (HPLC) as given below. The intermediate was then reduced to the cationic complex ^{99m}Tc-Q3 ($[^{99m}Tc(III)(acac_2en)(TMPP)_2]^+$) by anaerobic addition of tris(3-methoxy-1-propyl)phosphine (TMPP) hydrochloride (0.1 ml of 50 mg/ml solution in ethanol) and heating at 80–90°C for 10 min.

Purification was necessary to remove excess ligands prior to patient injection. The crude ^{99m}Tc-Q3 preparation was diluted to 20 ml with water and loaded onto a preconditioned Waters C18 Sep-Pak Plus cartridge. The Sep-Pak was rinsed with 20 ml of water and then with 4 ml of 80% ethanol/20% water. The purified radiopharmaceutical was then eluted with 2 ml of 80% ethanol/20% saline, collecting the middle 1-ml fraction, filtered through a 0.2-μm filter, and finally diluted with 4 ml of sterile saline.

Quality control was performed by reversed-phase HPLC on a Hamilton 150 mm × 4.1 mm PRP^{-1} column using a mobile phase of 90% methanol/10% 0.01 *M* ammonium acetate at a flow rate of 1.0 ml/min. The radioactivity was monitored by a Beckman Model 170 radioisotope detector. The chromatograms were recorded and integrated using a Shimadzu Chromatopac C-R3A integrator. A radiochemical purity above 85% was considered acceptable for patient injection. Clinical preparations of ^{99m}Tc-Q3 were tested for bacterial endotoxin levels using the Limulus amebocyte lysate technique and for sterility using both trypticase soy broth and fluid thioglycollate medium; results of both tests were available on a posthoc basis. Bacterial endotoxins for all preparations were below the minimum detectable level of 0.31 EU/ml. Sterility tests were negative for 25 preparations, and tests for two preparations showed growth of nonpathogenic bacteria probably introduced during inoculation of the culture medium.

In 27 clinical preparations of ^{99m}Tc-Q3, the radiochemical purity of the final ^{99m}Tc-Q3 complex was 96.0% ± 3.6% (mean ± s.d.); the radiochemical purity of the intermediate Tc(V) complex was 78.8% ± 12.3% (n = 20). The radiochemical yield (not corrected for radioactive decay) varied from 31.3% to 55.2% with an average of 40.7%. Technetium-99m-Q3 preparations were relatively stable. The decomposition rate determined for 10 batches at times from 2 to 24 hr after preparation averaged 2.3%/hr. The only decomposition product observed was ^{99m}Tc pertechnetate.

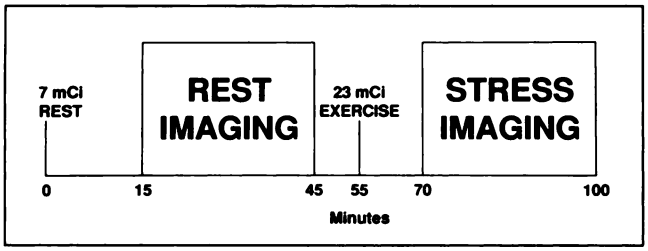

FIGURE 1. Rest and exercise ^{99m}Tc-Q3 imaging protocol.

Exercise ^{99m}Tc-Q3 Tomography

Resting and exercise ^{99m}Tc-Q3 imaging was performed at least 2 days before or after ^{201}Tl imaging in each study participant (mean 16 ± 6 days). Using the same gamma camera and nuclear medicine computer utilized in the thallium studies, the ^{99m}Tc-Q3 studies were performed with a high-resolution technetium collimator. The gamma camera photopeak was centered around the 140-keV gamma energy of ^{99m}Tc with a 20% window. The rest-exercise ^{99m}Tc-Q3 imaging protocol was designed to permit completion of the entire test sequence within 100 min (Fig. 1). In the fasting state, 5–7 mCi of ^{99m}Tc-Q3 was injected at rest and tomographic imaging was started 15 min later. On completion of tomographic imaging, the patient underwent the same graded exercise sequence used for thallium imaging. At the same exercise heart rate used for thallium administration, 20–23 mCi of ^{99m}Tc-Q3 was injected and exercise continued for an additional 1 min. Technetium-99m-Q3 imaging was started 15 min following tracer injection (*19*). Tomographic data were acquired with the same acquisition parameters used for ^{201}Tl imaging except as noted previously. Tomographic filtering, data reconstruction and display on radiographic film employed the same methods described for ^{201}Tl imaging.

Heart-to-Organ Ratio Calculation

Heart-to-organ radioactivity ratios were calculated by a modification of the method of Wackers et al. (*3*). All data were calculated from the anterior plane projection from each tomographic acquisition from the six healthy volunteers. Thus, heart-to-organ ratios were determined at 20 min following resting ^{99m}Tc-Q3 injection, 20 min following exercise ^{99m}Tc-Q3 injection, 20 min following exercise ^{201}Tl injection, and at rest 3.5 hr following ^{201}Tl injection. A region of interest (ROI) was placed around the entire left ventricular myocardium and the mean number of counts per pixel was calculated. A 3 × 3-pixel ROI was placed over the hepatic margin adjacent to the inferoapical wall of the left ventricle. A 3 × 3-pixel ROI was placed over the left lung adjacent to the anterolateral left ventricular wall. The heart-to-liver ratio was calculated as the mean myocardial activity per pixel divided by the mean hepatic activity per pixel. Heart-to-lung activity was calculated as the mean myocardial activity per pixel divided by the mean pulmonary activity per pixel. Differences in heart-to-liver or heart-to-lung ratios with ^{201}Tl and ^{99m}Tc-Q3 were tested for statistical significance with a repeated measures analysis of variance followed by Scheffe's F-test.

Interobserver variability in the calculation of heart-to-organ ratios was determined by two independent operators. Each operator determined heart-to-liver ratios from rest and exercise images for each of the six healthy volunteers. For the 12 pairs of heart-to-liver ratio determinations, the correlation coefficient was 0.92.

Coronary Arteriography

Coronary arteriography was performed by the Judkins technique with visualization of each coronary artery in multiple orthogonal projections. A 50% reduction in luminal diameter of the artery or its major branch was considered to be angiographically significant. All angiograms were interpreted by an experienced angiographer without knowledge of the ^{99m}Tc-Q3 image findings.

Data Analysis

The treadmill electrocardiogram was interpreted by standard criteria (*20*). The ^{201}Tl and ^{99m}Tc-Q3 images were interpreted in a qualitative manner by two readers who were blinded to all patient data except for patient gender, height and weight. Disagreement as to overall normalcy of the study was resolved by a third reader blinded to study conditions. Assignment of a myocardial perfusion defect to the distribution of a single coronary artery followed a previously validated template (*21*). In this scheme, the septum and anterior wall are in the distribution of the left anterior descending artery, the lateral wall is in the left circumflex distribution, and the inferior and posterior walls are in the distribution of the right coronary artery. For this study, perfusion defects located in the apex of the left ventricle were considered to be consistent with but not specific for the distribution of any single coronary artery. A perfusion defect on postexercise images showing no evidence of improvement on rest, redistribution or reinjection images was classified as a fixed defect. A perfusion defect on postexercise images that showed improved tracer activity on rest, redistribution or reinjection images was classified as a redistributing defect. Differences in sensitivity, normalcy rate or accuracy between radiotracers were tested by McNemar's test. A p value <0.05 was considered to demonstrate statistical significance. For subsequent analysis of noninvasive test accuracy, the two patients without angiographic CAD were considered together with the six healthy volunteers to form a group of eight "normals".

RESULTS

Exercise Electrocardiographic Results

Each of the 21 study participants completed two exercise electrocardiograms—one in conjunction with ^{201}Tl injection and one with ^{99m}Tc-Q3 injection. Results of the exercise tests are given in Table 1.

Heart-to-Organ Radioactivity Ratios

Heart-to-liver and heart-to-lung radioactivity ratios for ^{99m}Tc-Q3 and ^{201}Tl are shown in Table 2. Resting heart-to-liver ratios, as calculated at the hepatic margin adjacent to the inferoapical myocardial wall, tended to be lower for ^{99m}Tc-Q3 compared to ^{201}Tl, but the differences were not statistically significant. The postexercise mean heart-to-liver ratio was significantly greater for ^{201}Tl compared to ^{99m}Tc-Q3. The exercise ^{201}Tl mean heart-to-liver ratio was also significantly greater than the mean resting heart-to-liver ratio. The heart-to-liver ratio for ^{99m}Tc-Q3 was not significantly different at exercise when compared to rest. This may have resulted in part from the presence of residual hepatic activity from the rest ^{99m}Tc-Q3 injection at the time of exercise imaging. Heart-to-lung activity ratios were similar for ^{201}Tl and for ^{99m}Tc-Q3 both at rest and following exercise. In general, lung activity was low for both radiopharmaceuticals.

TABLE 1
Exercise Electrocardiographic Results

	Patients with known or suspected coronary disease (n = 21)		Volunteers (n = 6)	
	^{201}Tl	^{99m}Tc-Q3	^{201}Tl	^{99m}Tc-Q3
Exercise duration(s)	321 ± 50	345 ± 47	768 ± 68	738 ± 72
Tracer injection heart rate (bpm)	124 ± 5	125 ± 4	177 ± 3	179 ± 4
Peak exercise heart rate (bpm)	132 ± 5	130 ± 5	185 ± 4	183 ± 4
Peak exercise systolic blood pressure (mmHg)	160 ± 5	164 ± 3	173 ± 6*	153 ± 6*
Peak exercise diastolic blood pressure (mmHg)	82 ± 2	84 ± 2	83 ± 2	80 ± 2
Chest pain with exercise (number of patients)	2	4	0	0
ST segment result				
Abnormal	3	3	0	0
Normal	4†	4†	6	6
Nondiagnostic	14	14	0	0

*$p < 0.05$.
†Includes the two patients with no angiographically significant CAD.

Myocardial Perfusion Imaging—Qualitative Interpretation

Representative examples of exercise and rest ^{201}Tl and ^{99m}Tc-Q3 images from a healthy volunteer are shown in Figure 2. Examples of exercise and rest ^{201}Tl and ^{99m}Tc-Q3 images from a patient with an occluded left anterior descending coronary artery are shown in Figure 3. The short-axis ^{99m}Tc-Q3 images delineate the anterior, septal and inferior extent of the reversible ischemic defect. Adjacent hepatic activity on the rest ^{99m}Tc-Q3 images is also evident. On the horizontal long-axis images from the same patient, the extent and severity of the apical perfusion defect are shown.

By qualitative analysis, 16 of 19 patients with angiographic CAD had a corresponding regional perfusion abnormality on ^{99m}Tc-Q3 imaging (sensitivity equals 84%) and 13 of 19 patients had a corresponding ^{201}Tl perfusion defect (sensitivity equals 68%, p = ns versus Q3 sensitivity). Each of the eight normal subjects had a normal ^{99m}Tc-Q3 scan and a normal ^{201}Tl scan (normalcy rate equals 100%). Detection of stenoses in individual coronary arteries by qualitative analysis of myocardial perfusion images is shown in Table 3. Technetium-99m-Q3 and ^{201}Tl imaging provided comparable sensitivities and normalcy rates for disease detection in each of the three coronary arterial distributions. Overall, there was agreement between ^{99m}Tc-Q3 interpretation and ^{201}Tl image interpretation regarding the presence or absence of a perfusion defect in 140 of 162 myocardial segments (86%, kappa statistic = 0.63).

An assessment of defect reversibility was made from the myocardial perfusion tomograms in each left ventricular segment with ^{201}Tl and ^{99m}Tc-Q3. For the 27 study participants, six myocardial segments (septal, anterior, lateral, inferior, posterior and apical) were assessed on each study and interpreted by two independent readers. Thus, a total of 324 myocardial segment evaluations were available for each radiopharmaceutical. For ^{201}Tl, 33 reversible and 27 fixed myocardial perfusion defects were reported (19% of all segments). With ^{201}Tl imaging, reversibility of a segmen-

TABLE 2
Heart-to-Organ Ratios for Technetium-99m-Q3 and Thallium-201

	Heart-to-Liver		Heart-to-Lung	
	Rest	Exercise	Rest	Exercise
^{99m}Tc-Q3	0.67 ± 0.06‡	0.94 ± 0.06*	1.82 ± 0.09	1.88 ± 0.08
^{201}Tl	1.21 ± 0.09†	2.06 ± 0.15*†	1.81 ± 0.12	2.33 ± 0.18

*†$p < 0.05$, n = 6 subjects.
‡p = ns vs. ^{201}Tl at rest, 3.5 hr after injection.
Technetium-99m-Q3 ratios were obtained 20 min after injection. Exercise thallium ratios were obtained 20 min after injection. Rest thallium ratios were obtained 3.5 hr after injection.

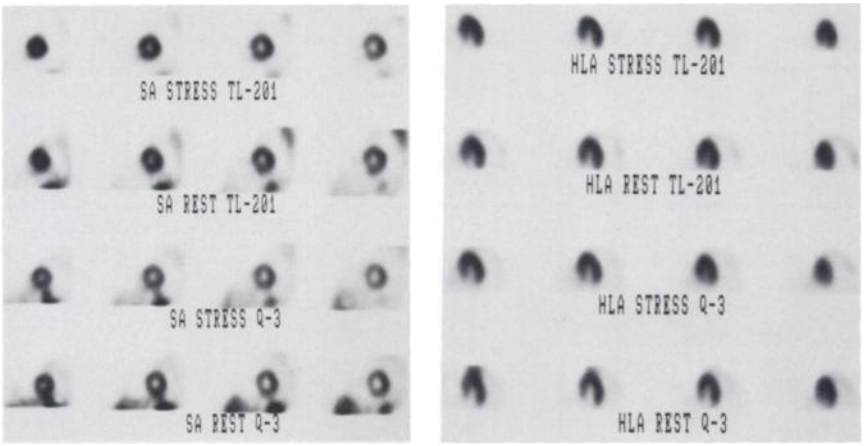

FIGURE 2. Representative short-axis (left panel) and horizontal long-axis (right panel) tomographic images acquired following ^{201}Tl injection with exercise (top row) and at rest (second row) in a healthy volunteer. Corresponding ^{99m}Tc-Q3 exercise (third row) and rest images (fourth row) are shown for the same volunteer.

tal perfusion defect was reported in 55% of abnormally perfused segments. For ^{99m}Tc-Q3, 32 reversible defects and 37 fixed defects were reported (21% of all segments). With ^{99m}Tc-Q3 imaging, reversibility of a segmental perfusion defect was reported in 46% of abnormally perfused segments (p = ns, kappa statistic = 0.19 for defect reversibility by ^{201}Tl versus ^{99m}Tc-Q3). Two study patients had fixed perfusion defects only based on ^{99m}Tc-Q3 images but had evidence of reversible ischemia on the corresponding ^{201}Tl images. Conversely, one patient with fixed perfusion defects only based on ^{201}Tl images had evidence of reversible ischemia on the corresponding ^{99m}Tc-Q3 images.

Interobserver agreement was present in 24 of 27 thallium studies (89%) and 25 of 27 ^{99m}Tc-Q3 studies (93%). Interobserver agreement concerning the presence or absence of a perfusion defect in an individual myocardial segment occurred in 141 of 160 segments (88%) with ^{201}Tl and in 139 of 160 segments (87%) with ^{99m}Tc-Q3 (p = ns versus ^{201}Tl). Of 67 left ventricular myocardial segments identified by both readers as containing a perfusion defect with exercise, there was interobserver agreement regarding defect reversibility in 28 of 36 segments (78%) imaged with ^{201}Tl and in 25 of 31 segments (81%) imaged with ^{99m}Tc-Q3 (p = ns versus ^{201}Tl).

DISCUSSION

Technetium-99m-Q3 is a mixed-ligand imaging agent that provides prompt myocardial visualization and rapid hepatic clearance. In the present study which used a rest and exercise sequence that could be completed in less than 100 min, ^{99m}Tc-Q3 permitted overall detection of CAD and detection of individual coronary artery stenoses with an accuracy comparable to that of ^{201}Tl. Technetium-99m myocardial imaging agents currently available for clinical use have provided improved myocardial image clarity compared to ^{201}Tl but have been limited by cardiac overlap from prominent hepatic activity early after tracer injection (*3–8*). In the present study, heart-to-liver ratios of ^{99m}Tc-Q3 activity acquired 20 min following Q3 injection at rest compared favorably to corresponding 60-min postinjection ratios for ^{99m}Tc-sestamibi reported in the literature (*3*). This confirmed the subjective impression that resting ^{99m}Tc-Q3 tomograms acquired beginning 15 min following radiopharmaceutical injection were not substantially degraded by scattered photons from ^{99m}Tc-Q3 distributed in organs located below the diaphragm.

Studies of ^{99m}Tc-Q3 in an open-chest, anesthetized canine model have shown a high correlation of myocardial ^{99m}Tc-Q3 activity to actual myocardial blood flow over a

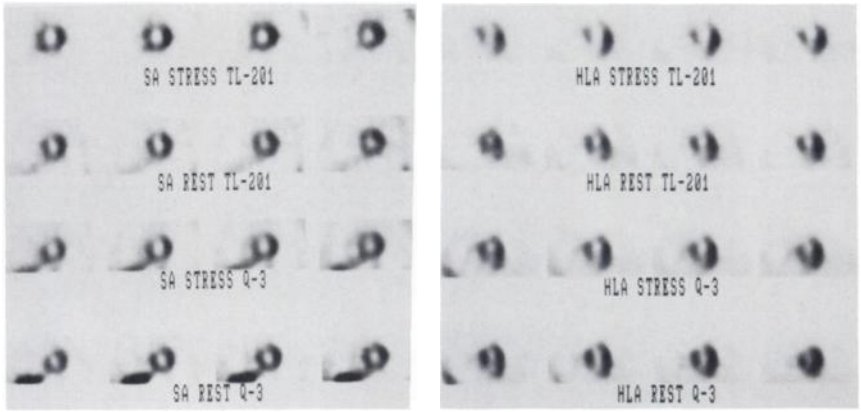

FIGURE 3. Short-axis (left panel) and horizontal long-axis (right panel) tomographic slices from a 63-yr-old man with proximal occlusion of the left anterior descending coronary artery and collateral filling from the right coronary artery. Exercise and rest images following ^{201}Tl injection are shown in the top two rows. Exercise and rest images following ^{99m}Tc-Q3 injection are shown in the lower two rows.

TABLE 3
Detection of CAD and Stenosis in Individual Coronary Vessels by Qualitative Methods

	^{201}Tl		^{99m}Tc-Q3	
	Sensitivity	Normalcy Rate	Sensitivity	Normalcy Rate
CAD	13/19 (68%)	8/8 (100%)	16/19 (84%)	8/8 (100%)
LAD	7/9 (78%)	17/18 (94%)	8/9 (89%)	16/18 (89%)
LCX	5/11 (45%)	14/16 (88%)	4/11 (36%)	15/16 (94%)
RCA	6/14 (43%)	12/13 (92%)	11/14 (79%)	13/13 (100%)

p = NS for all comparisons of ^{201}Tl vs. ^{99m}Tc-Q3. CAD = overall detection of the presence or absence of CAD; LAD = left anterior descending artery; LCX = left circumflex artery; RCA = right coronary artery.

flow range of 0 to 2.0 ml/g/min as measured by microsphere methods (*14*). In an open-chest, anesthetized canine model, in which reduced flow through the left circumflex artery was maintained constant over 4 hr and intravenous dipyridamole was administered to augment left anterior descending artery flow at the time of ^{99m}Tc-Q3 administration, no evidence of ^{99m}Tc-Q3 redistribution was observed over 4 hr (*14*). There have been few previous accounts of ^{99m}Tc-Q3 administration in humans (*12,22,23*). Rossetti et al. (*22*) administered a single dose of ^{99m}Tc-Q3 to six healthy volunteers in order to determine whole-body biodistribution. Blood clearance was rapid and followed by prompt tracer clearance through the hepatobiliary system. These authors also described ischemic and infarcted regions on ^{99m}Tc-Q3 tomographic images in eight patients with angiographically documented CAD (*22*). Bisi et al. (*23*) administered ^{99m}Tc-Q3 to three patients at rest and performed tomographic imaging 2 hr later. Subsequently, ^{99m}Tc-labeled microspheres were injected into the coronary arteries at the time of coronary arteriography and tomographic imaging was repeated. The regional distribution of ^{99m}Tc-Q3 correlated with the distribution of the ^{99m}Tc-labeled microspheres.

In the present study, the myocardial tomograms acquired following ^{99m}Tc-Q3 injection were of excellent technical quality and compared favorably to the corresponding ^{201}Tl tomograms. By subjective evaluation, ^{99m}Tc-Q3 and ^{201}Tl imaging provided comparable assessment for the presence or absence of CAD and for detection of individual coronary artery stenoses. In addition, there was good interobserver agreement in the interpretation of ^{99m}Tc-Q3 images—comparable to that obtained with ^{201}Tl. With the exception of photopeak and collimator selection, the imaging methods and tomographic data filtering procedures used for ^{99m}Tc-Q3 images were those previously optimized for ^{201}Tl tomographic imaging. It is likely that image acquisition and processing methods can be further improved to optimize ^{99m}Tc-Q3 images. Previous studies (*24,25*) have shown that reversible myocardial defects on exercise, redistribution and reinjection ^{201}Tl images predict improvement in left ventricular regional wall motion following a revascularization procedure. However, Cuocolo et al. (*26*) found fewer reversible segmental perfusion defects with rest and exercise injections of ^{99m}Tc-sestamibi compared to the number of reversible defects on exercise, redistribution and reinjection ^{201}Tl images in the same patients. In the present study, defect reversibility was observed in 55% of perfusion defect interpretations using exercise and reinjection ^{201}Tl imaging and in 46% of perfusion defect interpretations using separate rest and exercise ^{99m}Tc-Q3 injections. The difference was not statistically significant. It has been shown that mild or moderate fixed ^{201}Tl defects usually contain viable myocardium (*27,28*). In a preliminary report, Arrighi et al. (*29*) found that classification of fixed ^{99m}Tc-sestamibi defects as mild, moderate or severe could improve detection of viable myocardium. This type of approach may also improve assessment of myocardial viability with ^{99m}Tc-Q3 in future studies.

Potential limitations of the present study require comment. In previous studies of new ^{99m}Tc radiopharmaceuticals, planar imaging was generally used (*3*) and heart-to-organ ratios were calculated from planar anterior images containing a large number of scintigraphic events. In this tomographic study of ^{99m}Tc-Q3, the heart-to-organ ratios were calculated from the anterior plane of the tomographic sequence. Although the number of scintigraphic events was lower than those obtained from a standard planar anterior image, the interobserver and intraobserver variability in calculation of heart-to-organ ratios was low. Comparability of heart-to-organ ratios calculated from tomographic anterior projections and from standard anterior planar acquisitions is further illustrated by the similar ratios for ^{201}Tl using the former method in the present study and the latter method in the study of Wackers et al. (*3*).

The principal limitation of this initial study of ^{99m}Tc-Q3 is the small size of the study population. The trend toward higher sensitivity for detection of CAD with ^{99m}Tc-Q3 compared to ^{201}Tl imaging was not statistically significant. Larger studies with increased statistical power would be required to demonstrate conclusively that the higher number of correct diagnoses with ^{99m}Tc-Q3 compared to ^{201}Tl imaging was not due to chance alone. In addition, further basic investigation is needed to clarify the mechanism by which ^{99m}Tc-Q3 is taken up and retained by myocytes.

We conclude that rest and exercise ^{99m}Tc-Q3 injection imaging provides high quality myocardial images with di-

agnostic accuracy for detection of CAD and individual coronary artery stenoses comparable to that of ^{201}Tl. In addition, a favorable early ratio of heart-to-liver activity following ^{99m}Tc-Q3 administration suggests that a relatively condensed imaging sequence may be possible. Further investigation of ^{99m}Tc-Q3 is justified.

ACKNOWLEDGMENT

Supported in part by grant HL 21276-14 from the National Heart, Lung, and Blood Institute, National Institutes of Health, Bethesda, Maryland.

REFERENCES

1. Deutsch E, Bushong W, Glavan KA, et al. Heart imaging with cationic complexes of technetium. *Science* 1981;214:85–86.
2. Gerson MC, Deutsch EA, Nishiyama H, et al. Myocardial perfusion imaging with ^{99m}Tc-DMPE in man. *Eur J Nucl Med* 1983;8:371–374.
3. Wackers FJTh, Berman DS, Maddahi J, et al. Technetium-99m-hexakis 2-methoxyisobutyl isonitrile: human biodistribution, dosimetry, safety, and preliminary comparison to thallium-201 for myocardial perfusion imaging. *J Nucl Med* 1989;30:301–311.
4. Taillefer R, Lambert R, Essiambre R, Phaneuf DC, Leveille J. Comparison between thallium-201, technetium-99m-sestamibi and technetium-99m-teboroxime planar myocardial perfusion imaging in detection of coronary artery disease. *J Nucl Med* 1992;33:1091–1098.
5. Seldin DW, Johnson LL, Blood DK, et al. Myocardial perfusion imaging with technetium-99m-SQ30217: comparison with thallium-201 and coronary anatomy. *J Nucl Med* 1989;30:312–319.
6. Hendel RC, McSherry B, Karimeddini M, Leppo JA. Diagnostic value of a new myocardial perfusion agent, teboroxime (SQ 30,217), utilizing a rapid planar imaging protocol: preliminary results. *J Am Coll Cardiol* 1990;16: 855–861.
7. Li Q-S, Solot G, Frank TL, Wagner HN Jr, Becker LC. Tomographic myocardial perfusion imaging with technetium-99m-teboroxime at rest and after dipyridamole. *J Nucl Med* 1991;32:1968–1976.
8. Iskandrian AS, Heo J, Nguyen T, Mercuro J. Myocardial imaging with Tc-99m-teboroxime: technique and initial results. *Am Heart J* 1991;121: 889–894.
9. Higley B, Smith FW, Smith T, et al. Technetium-99m-1,2-bis[bis(2-ethoxyethyl)phosphino]ethane: human biodistribution, dosimetry and safety of a new myocardial perfusion imaging agent. *J Nucl Med* 1993;34:30–38.
10. Kelly JD, Forster AM, Higley B, et al. Technetium-99m-tetrofosmin as a new radiopharmaceutical for myocardial perfusion imaging. *J Nucl Med* 1993;34:222–227.
11. Jain D, Wackers FJTh, Mattera J, McMahon M, Sinusas AJ, Zaret BL. Biokinetics of technetium-99m-tetrofosmin: myocardial perfusion imaging agent: implications for a one-day imaging protocol. *J Nucl Med* 1993;34: 1254–1259.
12. Rossetti C, Vanoli G, Paganelli G, et al. Evaluation in humans of a new tracer with optimized properties for myocardial perfusion imaging: [Tc-99m] Q12 [Abstract]. *Eur J Nucl Med* 1991;18:540.
13. Gerson MC, Millard RW, Roszell NJ, et al. Myocardial kinetics of Tc-99m Q12 in dogs [Abstract]. *Circulation* 1992;86(suppl I):I-708.
14. Gerson MC, Millard RW, McGoron AJ, et al. Myocardial uptake and kinetics of Tc-99m Q3 in dogs [Abstract #602]. Proceedings of the First International Congress of Nuclear Cardiology. Cannes, France, 1993.
15. De Rosch MA, Brodack JW, Grummon GD, et al. Kit development for the Tc-99m myocardial imaging agent TechneCard™ [Abstract]. *J Nucl Med* 1992;33:850.
16. Rohe RC, Thomas SR, Cummings DD, Deutsch EA, Gerson MC, Maxon HR. Organ uptake and biodistribution studies of Tc-99m-Q3, a new myocardial imaging agent [Abstract]. *J Nucl Med* 1993;34:156P.
17. Prigent FM, Maddahi J, Garcia E, et al. Thallium-201 stress-redistribution myocardial rotational tomography: development of criteria for visual interpretation. *Am Heart J* 1985;109:274–281.
18. Bruce RA, Kusumi F, Hosmer D. Maximal oxygen intake and nomographic assessment of functional aerobic impairment in cardiovascular disease. *Am Heart J* 1973;85:546–562.
19. Freidman J, Van Train K, Maddahi J, et al. "Upward creep" of the heart: a frequent source of false-positive reversible defects during thallium-201 stress-redistribution SPECT. *J Nucl Med* 1989;30:1718–1722.
20. Wilson RF, Marcus ML, Christensen BV, Talman C, White CW. Accuracy of exercise electrocardiography in detecting physiologically significant coronary arterial lesions. *Circulation* 1991;83:412–421.
21. Maddahi J, Van Train K, Prigent F, et al. Quantitative single photon emission computed thallium-201 tomography for detection and localization of coronary artery disease: optimization and prospective validation of a new technique. *J Am Coll Cardiol* 1989;14:1689–1699.
22. Rossetti C, Best T, Paganeli G, et al. Evaluation of a new nonreducible ^{99m}Tc(III) myocardial perfusion tracer: biodistribution and initial clinical experience [Abstract]. *J Nucl Med All Sci* 1990;34:223.
23. Bisi G, Lunghi F, Bacciottini L, et al. Preliminary clinical results with ^{99m}Tc-Q3: a new potential myocardial perfusion agent [Abstract]. *J Nucl Med All Sci* 1990;34:142–143.
24. Dilsizian V, Rocco TP, Freedman NMT, Leon MB, Bonow RO. Enhanced detection of ischemic but viable myocardium by the reinjection of thallium after stress-redistribution imaging. *N Engl J Med* 1990;323:141–146.
25. Ohtani H, Tamaki N, Yonekura Y, et al. Value of thallium-201 reinjection after delayed SPECT imaging for predicting reversible ischemia after coronary artery bypass grafting. *Am J Cardiol* 1990;66:394–399.
26. Cuocolo A, Pace L, Ricciardelli B, Chiariello M, Trimarco B, Salvatore M. Identification of viable myocardium in patients with chronic coronary artery disease: comparison of thallium-201 scintigraphy with reinjection and technetium-99m-methoxyisobutyl isonitrile. *J Nucl Med* 1992;33:505–511.
27. Dilsizian V, Freedman NMT, Bacharach SL, Perrone-Filardi P, Bonow RO. Regional thallium uptake in irreversible defects. Magnitude of change in thallium activity after reinjection distinguishes viable from nonviable myocardium. *Circulation* 1992;85:627–634.
28. Bonow RO, Dilsizian V, Cuocolo A, Bacharach SL. Identification of viable myocardium in patients with chronic coronary artery disease and left ventricular dysfunction. Comparison of thallium scintigraphy with reinjection and PET imaging with ^{18}F-fluorodeoxyglucose. *Circulation* 1991;83:26–37.
29. Arrighi JA, Diodati JG, Bacharach SL, Uddin S, Bonow RO, Dilsizian V. The detection of viable myocardium by Tc-99m sestamibi is enhanced when the severity of irreversible defects are assessed [Abstract]. *Circulation* 1992;86:I-108.